

Deep Contrastive One-Class Time Series Anomaly Detection

Rui Wang*, Chongwei Liu*, Xudong Mou*, Xiaohui Guo[†], Kai Gao[‡], Pin Liu*, Tianyu Wo[§], Xudong Liu*[†]

* School of Computer Science and Engineering, Beihang University, Beijing, China

[†] Hangzhou Innovation Institute, Beihang University, Hangzhou, China

[‡] University of New South Wales, Sydney, Australia

[§] College of Software, Beihang University, Beijing, China

{ruiking, liucw, mxd}@buaa.edu.cn; guoxh@act.buaa.edu.cn; kai.gao@unsw.edu.au; {liupin, woty, liuxd}@act.buaa.edu.cn

Abstract—The accumulation of time series data and the absence of labels make time-series Anomaly Detection (AD) a self-supervised deep learning task. Single-assumption-based methods may only touch on a certain aspect of the whole normality, not sufficient to detect various anomalies. Among them, contrastive learning methods adopted for AD always choose negative pairs that are both normal to push away, which is objecting to AD tasks’ purpose. Existing multi-assumption-based methods are usually two-staged, firstly applying a pre-training process whose target may differ from AD, so the performance is limited by the pre-trained representations. This paper proposes a deep Contrastive One-Class Anomaly detection method of time series (COCA), which combines the normality assumptions of contrastive learning and one-class classification. The key idea is to treat the representation and reconstructed representation as the positive pair of negative-samples-free contrastive learning, and we name it “sequence contrast”. Then we apply a contrastive one-class loss function composed of invariance and variance terms, the former optimizing loss of the two assumptions simultaneously, and the latter preventing “hypersphere collapse”. Extensive experiments conducted on four real-world time-series datasets show the superior performance of the proposed method achieves state-of-the-art. The code is publicly available at <https://github.com/ruiking04/COCA>.

Index Terms—contrastive learning, one-class classification, unsupervised learning, anomaly detection, time series

I. INTRODUCTION

Within cyber-physical systems, sensor-equipped devices generate a large volume of time-series data that contains massive status information, which provides the possibility of detecting unexpected errors and reducing maintenance costs in data-driven ways. Anomaly Detection (AD) plays an increasingly important role in this context. AD refers to detecting which data instances are significantly dissimilar to the majority [1], and is gradually being accomplished via deep learning-based methods due to the rapid growth of data and their outperforming of shallow methods [2]. However, in pursuit of the performance, deep methods have to be exposed to heavy supervision information, while singling out unexpected outlier from a large quantity of raw temporal data is costly, and ascertaining the time-series data labeling criterion is tricky. Therefore, current research generally considers AD as an unsupervised learning problem.

Xiaohui Guo (guoxh@act.buaa.edu.cn) is the corresponding author.

In terms of deep unsupervised AD methods, approaches of learning feature representations of “normality” usually graft anomaly scoring on off-the-shelf representations learning module in a little bit simple and crude way. Learning representation for discerning anomalies usually relies on some normality assumptions. For example, autoencoder-based [3], [4] and GANs-based methods [5], [6] assume normal samples are better restructured or generated from the latent space than abnormal ones. Similarly, one-class classification methods [7], [8] assume that the normal samples come from a single (abstract) class that could accurately describe the so-called “normality”. However, these normality assumptions may only touch on a certain aspect of the overall normality, some of which are just inspired by the pretext task of self-supervised representation learning. Meanwhile, there are various types of time series anomalies including point anomalies (global or local), subsequence anomalies and anomaly time series [9] (Fig 5), and it is not sufficient to detect anomalies by one normality assumption alone.

In particular, with the great success of contrastive learning in representation learning, several researchers use contrastive learning for AD. [10] directly treats the InfoNCE loss of CPC [11] as the anomaly score for image AD, performing the contrast of the context vector with the future representation vector. NeuTraL AD [12] devises a contrastive loss specific to a fixed set of learnable transformations and regards the training loss as the anomaly score, contrasting the transformed samples (views) with the original ones in the representation space. The contrastive learning AD methods above are based on a single assumption, that the comparison objects of normal samples have greater mutual information than those of anomalies. What makes it worse, they treat pairs of samples that are not transformed from the same normal one as negative pairs and push them away, even though both are normal. However, AD is actually to extract features common to the vast majority of normal samples, so the standard of choosing negative pairs leads to a decline in AD performance.

Indeed there are some scholars who combine these normality assumptions into some compound ones so as to learn more expressive representations for downstream anomaly detection. For instance, Deep SVDD [13] realizes a deep one-class classification framework for anomaly detection with deep fea-

tures or representations learned by a pre-trained autoencoder. [14] presents the two-stage one-class classifier on contrastive representations, and points out a subtle but important observation, i.e., the uniformity property of contrastive representation may hurt the one-class AD performance. It correspondingly discovers that a novel distribution level augmentation could remedy this defect to a large extent. Even though, we still argue that learning the normality representation is distinct from capturing the underlying data distribution governing the normality and outliers’ irregularity, and formally they are two discrepant optimization objectives. Therefore, with representation learning and outlier discriminating separated, the two-stage AD methods’ performance is limited. In addition, these AD methods are originally proposed in the computer vision domain, and generalizing them simply into time-series AD task is meaningless for their lack of temporal dependencies.

To address the above issues, we propose a one-stage negative-sample-free deep **Contrastive One-Class Anomaly (COCA)** detection model for time-series data. As shown in Fig 1, first, the original training data is augmented, making it easier to isolate anomalies from normal samples. Next, the augmented time series is encoded through a multi-layer temporal convolution neural network, and then put into a Seq2Seq model in the latent space to learn the critical characteristics of time series, temporal dependencies. The key to contrastive learning is to pull contrasting objects (positive pairs) closer in the representation space, and researchers use a variety of positive pairs, such as context/ future [11], different augmentations [15], and context/ mask [16]. Here, we regard the representation in the latent space and the representation reconstructed by the Seq2Seq model as positive pairs, and name it “sequence contrast”. Note that it’s different from an autoencoder, as the latter is a generative method, which performs the reconstruction of original data or so called pixel-level generation [15], carrying mass unnecessary details to downstream tasks. Finally, the positive pairs are fed to a learnable nonlinear projection layer to obtain their projections respectively.

The model is trained via a contrastive one-class loss function with two terms: *invariance* and *variance*. The invariance term is to maximize the cosine similarity between the one-class center, latent representations, and seq2seq outputs, and no need to adjust the hyper-parameter to balance the loss contribution of one-class and contrastive learning as in most multi-task learning. The variance term is borrowed from [17], [18], and the variance of the within-batch representations is maintained above a given threshold by hinge loss to avoid “hypersphere collapse” without negative sample pairs, which also solves the difficulty of identifying negative pairs in AD. In practice, the invariant term is treated as anomaly score for AD. In conclusion, COCA combines the two normality assumptions that latent and reconstructed representations 1) have greater mutual information and 2) belong to a single class, without requiring two-stage learning. We summarize our contributions as follows:

- A novel normality assumption that combines contrastive

learning and one-class classification is proposed for anomaly detection of time series.

- The sequence contrast is proposed for time series data, a new paradigm of contrastive learning. By analyzing the problem solved by contrastive learning, we clarify that its essence is the representation, neither the object of comparison nor the negative example.
- A novel contrastive one-class loss function including invariance and variance terms is proposed, to learn the classifier directly.
- The invariance term without any hyper-parameters can optimize both contrastive learning and one-class classification simultaneously, and its effectiveness has also been demonstrated in experiments.
- The variance term avoids the “hyperspherical collapse” problem in negative-sample-free contrastive learning and deep one-class classification.
- Extensive experiments of the proposed COCA framework are performed on four datasets, and the results show that COCA leads to a new state-of-the-art in time series anomaly detection.

II. RELATED WORK

This section contains a brief introduction of recent works in contrastive learning and deep anomaly detection.

Contrastive Learning. The recent renaissance of contrastive learning began with CPC [11], which proposed InfoNCE to pull positive samples closer to and push negative samples further from the original samples, but it relies on a large number of negative samples to learn a good representation. [19] summarizes two key properties of contrastive learning: 1) alignment: similar samples have similar representations (pull positive pair) and 2) uniformity: representations follow a uniform distribution on the hypersphere (push negative pair). On the one hand, PIRL [20] and MoCo [21] explore the storage and retrieval representations of a large number of negative samples to make the representations distributed on the hypersphere more uniformly. BYOL [22], SwAV [23], and SimSiam [24] achieve uniformity in contrastive learning without using negative samples. On the other hand, SimCLR [15] and TS-TCC [25] align augmented data representation to learn invariant representations for visual data and time series, respectively. Also, TS-TCC use temporal contrasting to address the temporal dependencies of time series. While all these contrastive learning approaches have successfully improved representation learning for visual data and time series, they could be unapplicable on time series anomaly detection. For example, contradictions exist between the uniformity of contrastive learning and the class imbalance of anomaly detection.

Deep Anomaly Detection. Recently, deep-learning for anomaly detection has been regarded as a new research frontier of the related field. Deep anomaly detection methods can roughly be divided into three categories: deep learning for feature extraction, learning feature representations of normality, and end-to-end anomaly score learning [2]. Deep learning

for feature extraction is two-staged learning that uses deep methods to learn representations for downstream anomaly detection. However, it does not directly address the anomaly detection task, so the representations learned in the pre-training may be detrimental to anomaly detection. Learning feature representations of normality couples representations learning with anomaly scoring in some way, such as autoencoder-based [3], [4], GANs-based [5], [6], predictability [26], [27], distance-based [28], [29], one-class classification-based [7], [8], clustering-based [30] and contrastive learning-based [10], [12] methods. The key to these methods lies in the assumption of normality/anomaly, and some assumptions of normality are inspired by the pretext task of self-supervised learning. For instance, GANs-based methods assume normal samples are better generated from the latent space of the generative network than anomalies. However, the normal sample assumption of these methods may explain only one aspect of overall normality, respectively. Uniquely, COCA does not resort to pre-training and organically integrates the normality assumption of one-class classification and contrastive learning to detect anomalies for time-series data.

III. METHODOLOGY

This section describes the proposed COCA in detail, including the structure, objective, and relation to contrastive learning.

A. Problem Definition

Given a set of time series $\mathcal{D} = \{\mathbf{X}_1, \mathbf{X}_2, \dots, \mathbf{X}_N\}$, $\mathbf{X}_i = \{x_1, x_2, \dots, x_T\}$ is a time series of length T , where $x_j \in \mathbb{R}^d$ is a d -dimensional vector. Because sliding windows are generally used to divide time series into length- T sequences, T is also called the sliding window length. $d = 1$ means that the time series is univariate, and $d > 1$ for multivariate. In time series AD, the anomaly score \mathbf{S}_i of \mathbf{X}_i is calculated by AD model such that the higher \mathbf{S}_i is, the more likely it is an anomalous time series.

B. Architecture

Fig. 1 shows the architecture of the COCA model. The time series \mathbf{X}_i from an augmented training set of the raw dataset is passed to a multi-layer temporal convolution feature encoder $f_\theta : \mathcal{X} \mapsto \mathcal{Z}$ which takes as input time series \mathbf{X}_i of length T and outputs latent representations z_1, \dots, z_L for L time-steps, potentially with a lower temporal resolution, i.e. $T > L$. They are then fed to a Seq2Seq encoder $g_\theta : \mathcal{Z} \mapsto \mathcal{C}$ to summarize all $z_{\leq L}$ as a context vectors c_L and then a Seq2Seq decoder $h_\theta : \mathcal{C} \mapsto \mathcal{Z}$ produce reconstruction representations z'_1, \dots, z'_L for L time-steps to learn temporal dependencies. Furthermore, latent representations z_k and seq2seq outputs z'_k are fed to a learnable nonlinear projector $p_\theta : \mathcal{Z} \mapsto \mathcal{Q}$ to output projections q and q' . The output of the projector is used to calculate the loss (III-C) to maximize the similarity between q and q' with respect to the one-class center $C_e \in \mathcal{Q}$ to combine the two normality assumptions: contrastive learning-based and one-class classification-based.

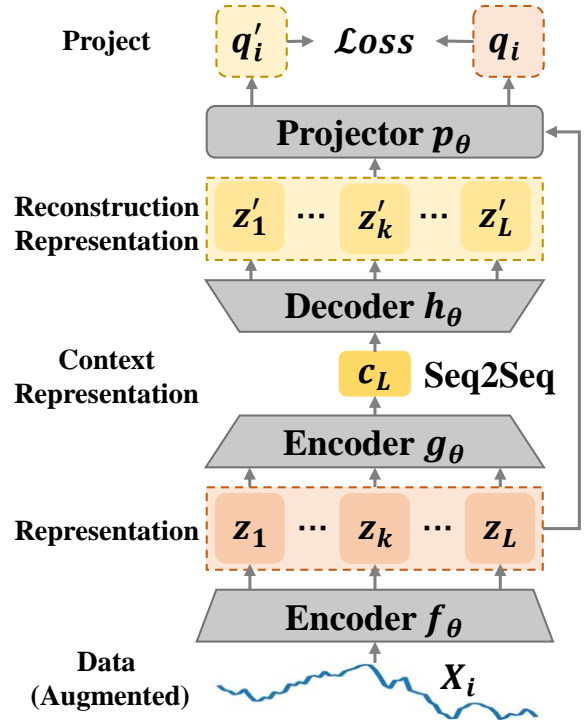


Fig. 1: Overall architecture of proposed COCA model.

Time-Series Augmentation. Data augmentation helps improve the performance of AD methods because it not only increases the volume of train data but also makes it easier to isolate anomalies [14], [31]. In this paper, jittering (noise addition) and scaling (pattern-wise magnitude change) are applied to expand the training set. Notably, the jittering and scaling hyper-parameters should be carefully chosen according to the nature of the time series anomalies. For example, an excessive jittering/ scaling rate may lead to local/ global point anomalies, both of which will degrade the anomaly detection performance in turn.

Feature encoder. The encoder network has a 3-block temporal convolutional architecture, each block comprising a Conv1D layer, a BatchNormalization (BN) layer, a ReLU activation function, and a MaxPool1D layer, where the first block also contains a Dropout layer. The time series input to the encoder should be normalized to zero mean and unit variance.

Seq2Seq. The Seq2Seq consists of an encoder and a decoder. The encoder is a 3-layer long short-term memory (LSTM) and the decoder is a 3-layer LSTM followed by a fully-connected (FC) layer. In this paper, the hidden space representation length $L < 20$, therefore LSTM can meet the needs of the context representation, while for long sequences, more recent advancements in Seq2Seq modeling such as self-attention networks or the Transformer model could help improve results further.

Projector. The projector uses a MLP with one hidden layer applied BN and ReLU to map representations to the space

where contrastive one-class loss is calculated.

C. The COCA Objective

The COCA objective consists of *invariance* and *variance* terms. The invariance term is to maximize the cosine similarity between the one-class center Ce , representations q_i , and seq2seq outputs q'_i in the projection space \mathcal{Q} , and the variance term avoids “hypersphere collapse” without negative sample pairs. Before explaining the invariance term of the COCA objective, it is necessary to state the optimization objectives of one-class classification and contrastive learning without negative pairs.

One-class classification. The optimization objective of Deep SVDD [13], a representative method for one classification, is defined as

$$\mathcal{L}_{svdd} = \frac{1}{N} \sum_{i=1}^N \|\phi(x_i, \Theta) - c\|^2, \quad (1)$$

where $c \in \mathcal{Z}$ is the one-class center, Θ is the set of parameters of a representation network ϕ . The last term is a weight decay regularizer. Deep SVDD obtains the sphere of the smallest volume by minimizing the \mathcal{L}_{svdd} in the representation space $\mathcal{Z} \subset \mathbb{R}^K$.

Negative-sample-free contrastive learning. BYOL [22], SimSiam [24], and Vicreg [17] are representatives of contrastive learning without negative pairs. The optimization objectives of BYOL and Vicreg are simplified as:

$$\mathcal{L}_{byol} = \frac{1}{N} \sum_{i=1}^N \|z_i - z'_i\|_2^2, \quad (2)$$

where z_i and z'_i are the representations of contrasting objects (positive pairs) in the latent space \mathcal{Z} . The optimization objectives of SimSiam is simplified as:

$$\mathcal{L}_{sim} = \frac{1}{N} \sum_{i=1}^N -\frac{z_i}{\|z_i\|_2} \cdot \frac{z'_i}{\|z'_i\|_2}. \quad (3)$$

Both Equation (2) and (3) are essentially pulling the positive pair close, while the difference is that the former uses Euclidean distance and the latter uses cosine similarity. As for the “hypersphere collapse” caused by no negative pairs, BYOL and SimSiam solve it by bootstrap and asymmetric networks, and Vicreg by variance.

Invariance term of COCA objective. A crude way to integrate one-class classification and contrastive learning is by treating it as multi-task learning with two adjustable hyper-parameters α and β as follows:

$$\alpha \cdot \mathcal{L}_{svdd} + \beta \cdot \mathcal{L}_{sim}. \quad (4)$$

The main intuition behind our model is that some correlation exists between one-class classification and contrastive learning, so that their objectives can be achieved simultaneously by a loss function without hyper-parameters α and β . Considering $\text{sim}(u, v) = u^T v / \|u\|_2 \|v\|_2$ denotes cosine similarity between

u and v , we define the invariance criterion d between ℓ_2 -normalized Q and Q' as

$$d(Q, Q') = \frac{1}{N} \sum_{i=1}^N \{[1 - \text{sim}(q_i, Ce)] + [1 - \text{sim}(q'_i, Ce)]\}, \quad (5)$$

where Ce is the ℓ_2 -normalized one-class center defined by:

$$Ce(Q, Q') = \frac{1}{2N} \sum_{i=1}^N (q_i + q'_i). \quad (6)$$

Here, Ce , q_i , and q'_i are distributed on the unit hypersphere after normalization. According to Equation (1), minimizing $d(Q, Q')$ brings q_i and q'_i closer to Ce , which clearly achieves one-class classification-based normality assumption. Meanwhile, on the unit hypersphere, $d(Q, Q')$ and \mathcal{L}_{sim} are related as follows:

$$d(Q, Q') \geq 1 + \mathcal{L}_{sim}(Q, Q'), \quad (7)$$

which becomes tighter as $d(Q, Q')$ decreases. Also, observe that minimizing the $d(Q, Q')$ shrinks an upper bound of contrastive errors $\mathcal{L}_{sim}(Q, Q')$, and achieves the contrastive learning-based normality assumption. For more details see next sub-section III-D.

For the case where a little bit of training data is anomalous, which is very common in AD tasks, the *soft-boundary invariance* of the COCA objective employing the hinge loss function is defined as:

$$d_{soft}(Q, Q') = L + \frac{1}{vN} \sum_{i=1}^N \max\{0, S_i - L\}, \quad (8)$$

where L is the $(1 - \eta)$ -quantile of S , η is a hyper-parameter, hyper-parameter $v \in (0, 1]$ controls the trade-off between L and violations of the boundary i.e. the amount of time series allowed to be mapped outside the boundary. S_i is the *anomaly score* of a time series \mathbf{X}_i , which is defined as:

$$S_i(\mathbf{X}_i) = 2 - \text{sim}(q_i, Ce) - \text{sim}(q'_i, Ce) \quad (9)$$

Variance term of COCA objective. In AD, COCA removes negative pairs in order to avoid performance degradation caused by pushing away negative pairs that are both normal. However, both of the negative-sample-free contrastive learning and Deep SVDD are likely to give an undesired trivial solution that all outputs “collapse” to a constant, i.e. “hypersphere collapse”. Inspired by [17], [18], COCA can then define the variance v as a hinge function on the standard deviation of the projected vectors q_i :

$$v(Q) = \frac{1}{N} \sum_{i=1}^N \max\left\{0, \gamma - \sqrt{\text{Var}(q_i) + \varepsilon}\right\}, \quad (10)$$

where γ is a constant target value of the standard deviation, and ε is a small scalar to prevent instabilities. In our experiments, γ is set to 1, ε is set to 10^{-4} . On the other hand, according to the research in Deep SVDD, selecting an appropriate one-class center can alleviate the problem of hypersphere collapse. In COCA, the one-class center Ce is

ensured to be non-zero in any dimension, and only updated in the first few epochs, because experiments show that an unfixed Ce would make the network easily converge to a trivial solution.

The overall loss function of COCA is a weighted average of the invariance and variance terms:

$$\mathcal{L} = \lambda d(Q, Q') + \frac{\mu}{2}(v(Q) + v(Q')), \quad (11)$$

where λ and μ are hyper-parameters controlling the contribution of each term in the loss. So similarly, when the training data contains a little bit anomalies, the *soft-boundary* loss function of COCA is defined as:

$$\mathcal{L}_{soft} = \lambda d_{soft}(Q, Q') + \frac{\mu}{2}(v(Q) + v(Q')). \quad (12)$$

Contrastive learning has two key properties: alignment and uniformity [19] (detail in II). There is an inverse relationship between uniformity and hypersphere collapse, the better the uniformity the less likely the collapse will occur, and vice versa. Nevertheless, uniformity somewhat contradicts the aim of one-class classification [14], because the latter is to bring representations closer to the center on the unit hypersphere, while some representations may be instead pulled far away by uniformity. Therefore, in our experiments, λ and μ are fixed to 1 and 0.1 respectively, to reduce the uniformity while prevent collapsing.

Anomaly Detection. In the test-phase, an anomaly score S_i will be generated for the time series \mathbf{X}_i . Then, the following formula is applied to determine whether \mathbf{X}_i can be classified as anomalies:

$$x_t = \begin{cases} anomaly, & S_i > \tau \\ normal, & S_i \leq \tau \end{cases}, \quad (13)$$

where τ is a predefined threshold.

The overall algorithm is summarized in Appendix A, as implemented with PyTorch.

D. Relation to Contrastive Learning

COCA treats representations q_i and reconstructed representations q'_i as positive pairs to learn shared information between different time steps of time series, discarding low-level information that is computationally expensive and unnecessary. Along with CPC [11], SimCLR [15], and wav2vec [16], though different in the types of positive pairs, COCA is essentially computing loss in the representation space. Therefore, maximizing the cosine similarity of q_i and q'_i in COCA is actually a type of negative-sample-free contrastive learning, and we name it sequence contrastive learning. For time series AD, COCA outperforms SimCLR-similar contrast methods that regard various augmentations as positive pairs, in the ablation experiments (IV-C).

Next, we will explain the mechanism of the invariance term to achieve the two normality assumptions. As shown in Fig. 2, on the unit hypersphere, the angle α is proportional to the Euclidean distance $l_{q_i, Ce}$ between two points. By optimizing the invariance term of the COCA objective defined in Equation (5), we are minimizing the cosine similarity between q_i , q'_i ,

and Ce , which is an upper bound on the sequence contrastive learning errors between q_i and q'_i . On the unit hypersphere, the formal proof is as follows:

$$\begin{aligned} d(q_i, q'_i) &= [1 - \text{sim}(q_i, Ce)] + [1 - \text{sim}(q'_i, Ce)] \\ &\propto \alpha + \beta \\ &\propto l_{q_i, Ce} + l_{q'_i, Ce} \\ &= \sqrt{\|q_i - Ce\|^2} + \sqrt{\|q'_i - Ce\|^2} \\ &\geq \sqrt{\|q_i - q'_i\|^2} \\ &\propto \gamma \\ &\propto 1 - \text{sim}(q_i, q'_i) \\ &= 1 + \mathcal{L}_{sim}(Q, Q'), \end{aligned} \quad (14)$$

here, l_* are the Euclidean distances. $\mathcal{L}_{sim}(Q, Q')$ is the contrastive error expressing the agreement between positive pairs. α , β and γ are related as follows:

$$\cos\gamma = \cos\alpha\cos\beta + \sin\alpha\sin\beta\cos\theta, \quad (15)$$

where θ is the dihedral angle. According to Equation (15), when $\alpha \rightarrow 0$ and $\beta \rightarrow 0$, $\cos\gamma \rightarrow 1$. Therefore, Equation (14) becomes tighter as $d(Q, Q')$ becomes smaller, which was also verified in our experiments.

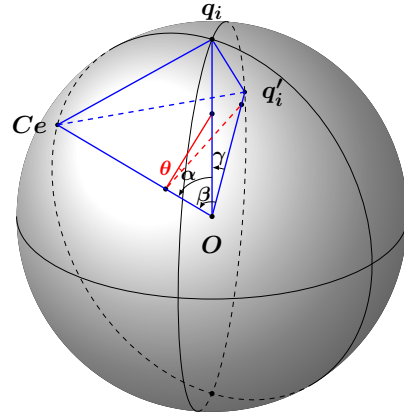


Fig. 2: Invariance term schematic. O is the center of the unit hypersphere, Ce is the l_2 -normalized one-class center, q_i and q'_i are l_2 -normalized vectors. θ is the dihedral angle between plane $CeOq_i$ and $CeOq'_i$, α and β are one-class errors, γ is the contrastive error.

IV. EXPERIMENTS

According to our research, COCA is the new state of the art technique in enhancing time series anomaly detection accuracy. The code is available at <https://github.com/ruiking04/COCA>.

A. Experimental Setup

Datasets. To evaluate the proposed model, four publicly accessible time-series datasets for anomaly detection are employed, comprising univariate and multivariate time series data

	NAB	AIOps	UCR	SMAP
Object	58	29	250	1
Domain	Various	Cloud KPIs	Various	Satellite
Real data	47	29	250	1
Variables	1	1	1	25
Length T	32	16	64	32
Total windows	11368	370155	302174	17587
Abnormal windows	10.15%	2.92%	0.60%	10.09%
Training split	15%	50%	30%	25%
Training Anomaly	7.64%	3.24%	0%	0%

Table I: Summary of time series anomaly detection datasets

from domains such as advertising, spacecraft telemetry, traffic, medical, and web services, among others. The datasets lie as follows.

- Numenta Anomaly Benchmark (**NAB**)¹. This is a collection of 58 labeled real-world and artificial time-series objects.
- AIOps challenge (**AIOps**)². This obtains 29 well-maintained business cloud KPIs from some large internet companies.
- 2021 SIGKDD multi-dataset time-Series anomaly detection competition³ / UCR time series anomaly detection (**UCR**)⁴ [32]. This contains 250 time-series objects from various fields.
- Soil Moisture Active Passive satellite (**SMAP**)⁵. This is multivariate real spacecraft telemetry time series data.

Table I summarizes these datasets. Note that an “object” mentioned means a time series containing thousands of time series samples. For example, UCR contains 250 objects, i.e., it consists of 250 time series from different sources, AD for each requires a model. The time series are partitioned into length- T sequences by a sliding window without overlap. The UCR dataset has the largest amount of data and the smallest percentage of anomalies, which is a challenge for some AD models. For the NAB dataset, we divide 15% of the data set as the training set to ensure that it contains fewer abnormal samples [33], while the other three datasets have been originally divided into training and test sets. The training sets of UCR and SMAP don’t contain anomalies, so the models are trained using Equation (11), while NAB and AIOps use *soft-boundary* loss function Equation (12).

Performance Metrics. In most cases, time series anomalies occur as continuous-time intervals rather than isolated points, leading to difficulty in determining how to quantify the predicted anomaly label sequence. Obviously, point-wise (PW) precision, recall, and F1-score are simple to compute, but not appropriate for anomalies of time windows. So far, there

have been three main metrics for time-series data anomaly detection: NAB Score [34], Point-Adjusted (PA) metrics [35], and Revised Point-Adjusted (RPA) metrics [36]. However, NAB Score is too complicated to be accepted widely. PA metrics assume that if any point in a ground truth anomaly window is identified as anomalous, all points in the window are evaluated as true positives. RPA metrics are based on the assumption that whenever any point in a ground truth anomaly window is tagged as anomalous, one true positive is recorded. A false negative would be reported for a positively labelled sequence if no predicted sequences overlap with it.

As is illustrated in Fig. 3, there are 10 contiguous time series ground truth with two anomaly segments in the first row. And under it lies the prediction anomaly scores of the 10 series. When the threshold of anomaly score is 0.5, PW F1-score is 0.36, PA F1-score is 0.62, and RPA F1-score is 0.4. PA is a winner-take-all strategy and is more tolerant of high false-positive rates, especially for long anomalies sequence. Although RPA metrics solve these problems, it penalizes false positives more severely, resulting in a low F1-score. In this paper, considering that each object of datasets vary in the sample quantity, we calculated F1-score based on RPA-adjusted true/false positive/negative counts of all time series objects in the whole dataset.

ground truth	0	1	1	1	1	0	0	1	1	1
anomaly score	0.7	0.2	0.7	0.9	0.3	0.3	0.7	0.2	0.4	0.1
PW metrics	1	0	1	1	0	0	1	0	0	0
PA metrics	1	1	1	1	1	0	1	0	0	0
RPA metrics	1	1			0	1	0			

Fig. 3: Illustration of PW, RA, and RPA metrics. 0 is normal and 1 is abnormal. The red boxes represent two anomalous sequences. The anomaly score threshold is 0.5.

B. Baselines and Implementation

Baselines. The proposed approach is compared against the following unsupervised and self-supervised anomaly detection methods.

Traditional Anomaly Detection Baselines. Three commonly traditional anomaly detection baselines are adopted: One-class SVM (OC-SVM) [37], Isolation Forest (IF) [38], and Random Cut Forest (RCF) [39].

Deep Anomaly Detection Baselines. Then, four deep anomaly detection methods: Deep one-class (Deep SVDD) [13], Spectral Residual CNN (SR-CNN) [40], Deep Autoencoding Gaussian Mixture Model (DAGMM) [30], and LSTM Encoder-decoder (LSTM-ED) [41].

Contrastive Learning Anomaly Detection Baselines. Finally, two contrastive learning baselines are set: Contrastive Predictive Coding Anomaly Detection (CPC-AD) [10] and

¹<https://github.com/numenta/NAB>

²http://iops.ai/competition_detail/?competition_id=5

³<https://compete.hexagon-ml.com/practice/competition/39/>

⁴https://www.cs.ucr.edu/~eamonn/time_series_data_2018/

⁵<https://github.com/khundman/telemanom>

	Assumption	Two stage	Original domain
Deep SVDD	Autoencoder&One-calss	✓	Image
SR-CNN	Saliency map	×	Time series
DAGMM	Clustering	×	Time series
LSTM-ED	Autoencoder	×	Time series
CPC-AD	Contrast	×	Image
TS-TCC-AD	Contrast&One-calss	✓	Time series

Table II: Summary of deep baselines.

Time Series Temporal and Contextual Contrasting Anomaly Detection (TS-TCC-AD) [14], [25].

For these deep baselines, Table II shows the normality assumptions, study domains, and whether two-staged. Although Deep SVDD and CPC-AD are originally targeted for image AD, their normality assumptions are relevant to this paper, so they were chosen as baselines. For Deep SVDD, we use Conv1D and LSTM to implement its autoencoder architecture in order to process time-series data. CPC is originally a method for sequential data, treating images as a sequence of pixels, so the network structure does not need to be changed significantly when processing time-series data. For TS-TCC-AD based on [14], TS-TCC [25] is used to learn the representation of time series in the pre-training phase and Deep SVDD is used for AD in the fine-tuning phase.

COCA Variants. Moreover, we include the following five COCA variants as baselines to demonstrate the effectiveness of individual components in COCA.

NoAug. The Variant NoAug removes the time-series augmentations of COCA.

NoOC. The Variant NoOC removes the one-class classification of COCA to optimize the similarity of representations q_i and reconstructed representations q'_i . Its invariance term of the loss function is defined as:

$$\frac{1}{N} \sum_{i=1}^N 1 - \text{sim}(q_i, q'_i). \quad (16)$$

NoCL. The Variant NoCL removes the contrastive learning of COCA to optimize the similarity of representations and one-class center. Its invariance term of the loss function is defined as:

$$\frac{1}{N} \sum_{i=1}^N 1 - \text{sim}(q_i, Ce). \quad (17)$$

The difference between the variant NoCL and Deep SVDD is that the former contains a learnable nonlinear projector p_θ network and no pre-training.

NoVar. The Variant NoVar removes the variance term of COCA to optimize the similarity of representations and one-class center. Its loss function is defined as:

$$d(Q, Q'). \quad (18)$$

COCA-vi. The variant COCA-vi treats different augmentations (jittering and scaling) as positive pairs for contrast

learning, similar to SimCLR [15]. Its invariance term of the loss function is defined as:

$$d(Z^1, Z^2), \quad (19)$$

where Z^1 and Z^2 are the representations of the time-series data after jittering and scaling, respectively.

Baseline	RPA F1			
	NAB	AIOps	UCR	SMAP
OC-SVM	14.84	21.20	0.05	17.10
IF	21.54	28.53	27.17	21.05
RCF	33.50±0.35	29.86±0.23	35.27±1.51	31.70±2.05
Deep SVDD	35.48±2.27	30.93±1.42	2.93±1.36	13.01±0.36
SR-CNN	15.76±1.03	34.84±0.83	13.97±0.01	-
DAGMM	8.27±3.20	13.62±2.68	0.01±0.00	10.39±5.23
LSTM-ED	21.55±0.21	31.96±2.09	49.35±1.02	20.99±2.85
CPC-AD	30.48±2.29	44.36±0.17	0.45±0.14	22.84±0.46
TS-TCC-AD	8.51±0.12	5.18±0.36	9.50±1.49	10.49±0.30
COCA	66.90±1.73	45.42±0.70	51.30±1.63	35.13±1.61
NoAug	65.82±2.01	43.62±2.06	43.15±2.75	33.32±2.79
NoOC	62.06±1.47	37.72±6.24	19.07±3.18	23.40±3.33
NoCL	64.76±1.73	45.90±0.88	44.19±2.09	30.63±4.03
NoVar	43.64±3.50	24.97±7.84	12.22±2.09	15.99±9.46
COCA-vi	62.92±2.05	43.68±0.83	39.12±2.71	25.55±5.55

Table III: Average RPA F1-score(%) with standard deviation for anomaly detection on time series datasets. Best results are in bold. The source code of SR-CNN does not support multivariate time series anomaly detection.

Implementation Details. The network structure of our proposed COCA consists of two parts: encoder and Seq2Seq. The encoder consists of 3-block temporal convolutional modules that each followed by batch normalization, ReLU activation, and 2×2 max-pooling. For the Seq2Seq, two identical three-layer LSTMs are employed with the same dropout rate at 0.45 as 1D-CNNs. As for optimizer, an Adam [42] optimizer with a learning rate from $1e-4$ to $5e-4$, weight decay of $5e-4$, $\beta_1 = 0.9$, and $\beta_2 = 0.99$ is adopted. Except for the UCR, after calculating the anomaly scores, COCA searches on anomaly sample rate p from 0.01% to 0.30% with step 0.01% to determine the optimal anomaly threshold τ . The UCR dataset has only one anomaly segment, so COCA directly takes the largest anomaly score as an anomaly. Note that the soft-boundary contrastive one-class loss function has been utilized to train models on NAB and AIOps datasets. In addition, COCA uses the early stopping strategy, as the dataset contains time series from different domains, especially NAB and UCR.

For a fair comparison, the same encoder architecture and embedding dimension are used for Deep SVDD, CPC-AD, TS-TCC, and COCA. Each method is run 10 times to obtain the mean and standard deviation. Lastly, the model is built with PyTorch 1.7 and Merlion 1.1.1⁶, and trained on a NVIDIA Tesla V100 GPU. In particular, Merlion is a machine learning

⁶<https://github.com/salesforce/merlion>

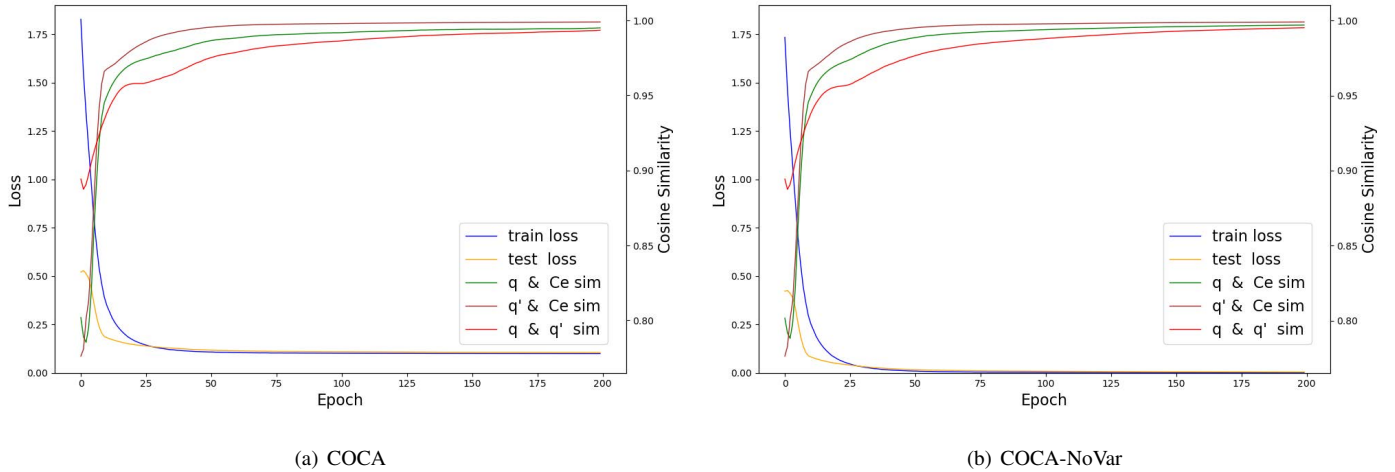


Fig. 4: Loss and cosine similarity results for COCA and COCA-NoVar on UCR. Blue: train loss, Orange: test loss, Green: $\text{sim}(q_i, Ce)$, Brown: $\text{sim}(q'_i, Ce)$, Red: $\text{sim}(q_i, q'_i)$.

library for time series anomaly detection [33]. For reproducibility, some crucial parameters are reported in Appendix B, and the baselines are reproduced in the source code ⁷.

C. Main Results

We conduct the F1-score evaluation metric based on the true/false positive/negative counts adjusted by PA and RPA, which is presented in Table III.

From the vertical view of the table, some methods perform poorly in UCR because there is only one anomaly segment in each time-series object, which leads to high false-positive rates. In particular, UCR was also used in [33] and their results were high, but we found that they recklessly fixed False Positive (FP) to 1 as long as anomalies were detected ⁸. On the other hand, the F1-score of all methods did not exceed 40% in the SMAP, indicating that multivariate time-series AD is more complex compared to univariate, and multivariate correlation needs to be considered.

From the horizontal view of the table, four conclusions can be drawn. First, in shallow methods, RCF with RPA F1-score over 30% performs well and even outperforms some deep methods, showing the classical shallow methods are worthwhile approaches to consider on some small datasets [43]. Second, LSTM-ED and Deep SVDD perform better than other deep baselines, indicating the normality assumptions of reconstruction and one-class classification are more relevant to the nature of AD. In addition, the performance of Deep SVDD could be limited by the pre-trained deep autoencoders. Last, the good performance of contrastive anomaly detection baselines (e.g., CPC-AD and TS-TCC-AD) shows that learning representations at high levels of semantics can discard some low-level information that is useless for AD. In sum, the COCA outperforms all baselines on four datasets, demonstrating the effectiveness of our method.

⁷<https://github.com/ruiqing04/COCA>

⁸https://github.com/salesforce/Merlion/blob/main/benchmark_anomaly.py

Also, Table III shows the effectiveness of each component in our proposed COCA model. Clearly, augmentations improve the performance of AD by more than $\sim 2\%$ on four datasets by analyzing the AD performance of the NoAug. For COCA, NoOC, and NoCL, the combination of multiple normality assumptions can effectively improve the performance of AD. Meanwhile, the NoVar performs poorly compared to COCA, which makes it clear that the variance term of the COCA objective is important. The COCA-vi is 5% averagely lower than the COCA on the four datasets because it treats different augmentations as positive pairs and ignores temporal dependencies. Overall, the results of COCA are better than the five variants, indicating the effectiveness and necessity of each component in our model.

D. Collapse and Relation to Contrastive Learning

To verify the validity of the invariant and variance terms in loss function of COCA, Fig. 4 illustrates loss and cosine similarity results for COCA and COCA-NoVar on UCR. As can be seen from Fig. 4(a), the process of optimizing the loss function \mathcal{L} makes $\text{sim}(q_i, Ce) \rightarrow 1$, $\text{sim}(q'_i, Ce) \rightarrow 1$ and $\text{sim}(q_i, q'_i) \rightarrow 1$, which indicates that the loss we design not only makes q_i and q'_i closer to Ce , but also minimizes the sequence comparison error $\text{sim}(q_i, q'_i)$. Comparing Fig. 4(a) and 4(b), it can be concluded that without the variance term, the loss \mathcal{L} drops rapidly to close to 0, implying that hypersphere collapse has occurred.

E. Visualization

To provide a more intuitive evaluation, visualizations of AD on NAB, AIOps, UCR, and SMAP are conducted, in Fig. 5. A point anomaly is a datum that behaves unusually when compared either to the other values in the time series (global) or to its neighboring points (local), and global point anomalies are also referred to as contextual anomalies [2]. A subsequence anomaly refers to anomalous consecutive points in time, wherein each of the individual points in isolation is

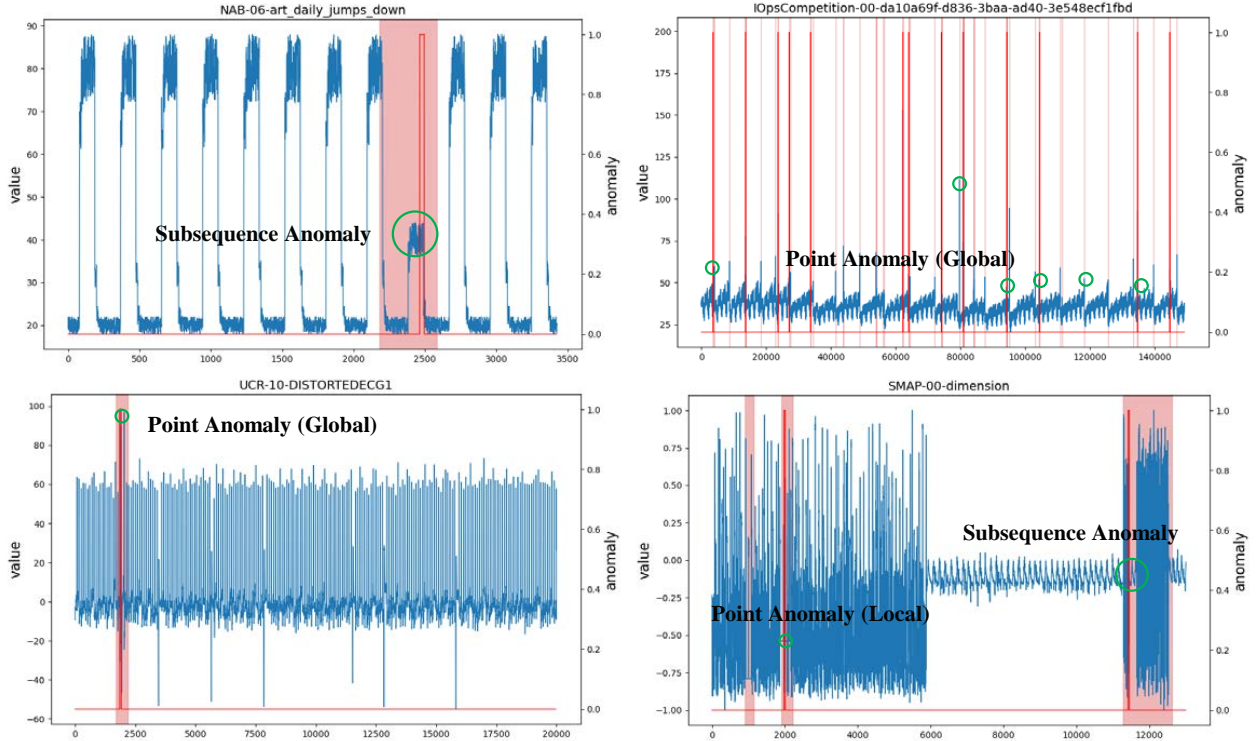


Fig. 5: AD results of COCA on NAB, AIOps, UCR, and SMAP datasets. The pink parts are the ground-truth anomalous fragments, and the red curves are the anomalies predicted by COCA (1 means anomaly, 0 means normality). The types of anomaly include point anomalies (global or local) and subsequence anomalies.

not necessarily a point anomaly. It can be seen that AIOps contains a large number of global point anomalies, which are suitable for some AD methods that are specialized in learning global features. In contrast, UCR, NAB, and SMAP contain both point and sequence anomalies. COCA performs well on NAB and UCR compared to on AIOps and further illustrates that AD methods combining multiple normality assumptions can be applied to complex anomalous situations.

F. Hyper-parameters Analysis

In this section, sensitivity analysis is performed on the NAB dataset to study two main parameters: $v \in (0, 1]$ in Equation (8) and the epoch e before stopping updating the center C_e . Fig. 6(a) shows the effect of v on the overall performance, where the y-axis is the RPA F1-score metric. Clearly, appropriate anomaly proportions v should be selected for different datasets since whether it is too large or too small will harm performance. For NAB, we observe that $v = 0.001$ is best. Fig. 6(b) shows the results of varying epoch e of stopping update center C_e in a range between 1 and 200. It's observed that the model performs best when $e = 10$, which implies that the center C_e should be frozen early, as updating the center C_e frequently makes the model more prone to hypersphere collapse.

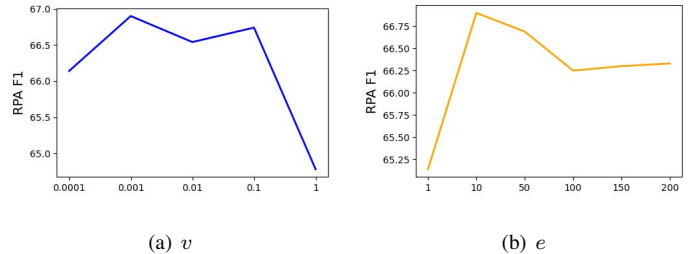


Fig. 6: Two sensitivity analysis experiments on NAB dataset. The left is the hyper-parameter $v \in (0, 1]$ of *soft-boundary invariance* and the right is training epoch e before stopping updating the center C_e .

V. CONCLUSION

We propose a novel deep framework called COCA for unsupervised time series anomaly detection. It combines the normality assumptions of contrastive learning and one-class classification, clarifies the essence of contrastive learning, and presents a new negative-sample-free type named “sequence contrast”. Specially, we present a novel contrastive one-class loss function optimizing the loss of both assumptions simultaneously in one stage without tuning hyperparameters as in most multi-task learning, as well as preventing “hypersphere collapse”. Experiments on various datasets demonstrate that

the performance of COCA achieves state-of-the-art. We hope our work can help deepen the understanding of contrastive learning and offer more possibilities for fusion studies of various anomaly detection methods.

ACKNOWLEDGMENT

The authors gratefully acknowledge support by the National Key Research and Development Program of China (2018YFB1306000).

REFERENCES

- [1] F. E. Grubbs, "Procedures for detecting outlying observations in samples," *Technometrics*, vol. 11, no. 1, pp. 1–21, 1969.
- [2] G. Pang, C. Shen, L. Cao, and A. V. D. Hengel, "Deep learning for anomaly detection: A review," *ACM Computing Surveys (CSUR)*, vol. 54, no. 2, pp. 1–38, 2021.
- [3] J. Chen, S. Sathe, C. Aggarwal, and D. Turaga, "Outlier detection with autoencoder ensembles," in *Proceedings of the 2017 SIAM international conference on data mining*. SIAM, 2017, pp. 90–98.
- [4] T. Kieu, B. Yang, C. Guo, and C. S. Jensen, "Outlier detection for time series with recurrent autoencoder ensembles," in *IJCAI*, 2019, pp. 2725–2732.
- [5] T. Schlegl, P. Seeböck, S. M. Waldstein, U. Schmidt-Erfurth, and G. Langs, "Unsupervised anomaly detection with generative adversarial networks to guide marker discovery," in *International conference on information processing in medical imaging*. Springer, 2017, pp. 146–157.
- [6] H. Zenati, C. S. Foo, B. Lecouat, G. Manek, and V. R. Chandrasekhar, "Efficient gan-based anomaly detection," *arXiv preprint arXiv:1802.06222*, 2018.
- [7] R. Chalapathy, A. K. Menon, and S. Chawla, "Anomaly detection using one-class neural networks," *arXiv preprint arXiv:1802.06360*, 2018.
- [8] P. Wu, J. Liu, and F. Shen, "A deep one-class neural network for anomalous event detection in complex scenes," *IEEE transactions on neural networks and learning systems*, vol. 31, no. 7, pp. 2609–2622, 2019.
- [9] A. Blázquez-García, A. Conde, U. Mori, and J. A. Lozano, "A review on outlier/anomaly detection in time series data," *ACM Computing Surveys (CSUR)*, vol. 54, no. 3, pp. 1–33, 2021.
- [10] P. de Haan and S. Löwe, "Contrastive predictive coding for anomaly detection," *arXiv preprint arXiv:2107.07820*, 2021.
- [11] A. v. d. Oord, Y. Li, and O. Vinyals, "Representation learning with contrastive predictive coding," *arXiv preprint arXiv:1807.03748*, 2018.
- [12] C. Qiu, T. Pfommer, M. Kloft, S. Mandt, and M. Rudolph, "Neural transforming learning for deep anomaly detection beyond images," *arXiv preprint arXiv:2103.16440*, 2021.
- [13] L. Ruff, R. Vandermeulen, N. Goernitz, L. Deecke, S. A. Siddiqui, A. Binder, E. Müller, and M. Kloft, "Deep one-class classification," in *International conference on machine learning*. PMLR, 2018, pp. 4393–4402.
- [14] K. Sohn, C.-L. Li, J. Yoon, M. Jin, and T. Pfister, "Learning and evaluating representations for deep one-class classification," *International Conference on Learning Representation (ICLR) 2021*, 2020.
- [15] T. Chen, S. Kornblith, M. Norouzi, and G. Hinton, "A simple framework for contrastive learning of visual representations," in *International conference on machine learning*. PMLR, 2020, pp. 1597–1607.
- [16] A. Baevski, Y. Zhou, A. Mohamed, and M. Auli, "wav2vec 2.0: A framework for self-supervised learning of speech representations," *Advances in Neural Information Processing Systems*, vol. 33, pp. 12 449–12 460, 2020.
- [17] A. Bardes, J. Ponce, and Y. Lecun, "Vicreg: Variance-invariance-covariance regularization for self-supervised learning," in *ICLR 2022-10th International Conference on Learning Representations*, 2022.
- [18] P. Chong, L. Ruff, M. Kloft, and A. Binder, "Simple and effective prevention of mode collapse in deep one-class classification," in *2020 International Joint Conference on Neural Networks (IJCNN)*. IEEE, 2020, pp. 1–9.
- [19] T. Wang and P. Isola, "Understanding contrastive representation learning through alignment and uniformity on the hypersphere," in *International Conference on Machine Learning*. PMLR, 2020, pp. 9929–9939.
- [20] I. Misra and L. v. d. Maaten, "Self-supervised learning of pretext-invariant representations," in *Proceedings of the IEEE/CVF Conference on Computer Vision and Pattern Recognition*, 2020, pp. 6707–6717.
- [21] K. He, H. Fan, Y. Wu, S. Xie, and R. Girshick, "Momentum contrast for unsupervised visual representation learning," in *Proceedings of the IEEE/CVF conference on computer vision and pattern recognition*, 2020, pp. 9729–9738.
- [22] J.-B. Grill, F. Strub, F. Altché, C. Tallec, P. Richemond, E. Buchatskaya, C. Doersch, B. Avila Pires, Z. Guo, M. Gheshlaghi Azar *et al.*, "Bootstrap your own latent—a new approach to self-supervised learning," *Advances in Neural Information Processing Systems*, vol. 33, pp. 21 271–21 284, 2020.
- [23] M. Caron, I. Misra, J. Mairal, P. Goyal, P. Bojanowski, and A. Joulin, "Unsupervised learning of visual features by contrasting cluster assignments," in *Thirty-fourth Conference on Neural Information Processing Systems (NeurIPS)*, 2020.
- [24] X. Chen and K. He, "Exploring simple siamese representation learning," in *Proceedings of the IEEE/CVF Conference on Computer Vision and Pattern Recognition*, 2021, pp. 15 750–15 758.
- [25] E. Eldele, M. Ragab, Z. Chen, M. Wu, C. K. Kwok, X. Li, and C. Guan, "Time-series representation learning via temporal and contextual contrasting," *IJCAI*, 2021.
- [26] D. Abati, A. Porrello, S. Calderara, and R. Cucchiara, "Latent space autoregression for novelty detection," in *Proceedings of the IEEE/CVF Conference on Computer Vision and Pattern Recognition*, 2019, pp. 481–490.
- [27] W. Liu, W. Luo, D. Lian, and S. Gao, "Future frame prediction for anomaly detection—a new baseline," in *Proceedings of the IEEE conference on computer vision and pattern recognition*, 2018, pp. 6536–6545.
- [28] M. Sugiyama and K. Borgwardt, "Rapid distance-based outlier detection via sampling," *Advances in Neural Information Processing Systems*, vol. 26, pp. 467–475, 2013.
- [29] G. Pang, L. Cao, L. Chen, and H. Liu, "Learning representations of ultrahigh-dimensional data for random distance-based outlier detection," in *Proceedings of the 24th ACM SIGKDD international conference on knowledge discovery & data mining*, 2018, pp. 2041–2050.
- [30] B. Zong, Q. Song, M. R. Min, W. Cheng, C. Lumezanu, D. Cho, and H. Chen, "Deep autoencoding gaussian mixture model for unsupervised anomaly detection," in *International conference on learning representations*, 2018.
- [31] I. Golan and R. El-Yaniv, "Deep anomaly detection using geometric transformations," in *Proceedings of the 32nd International Conference on Neural Information Processing Systems*, 2018, pp. 9781–9791.
- [32] H. A. Dau, E. Keogh, K. Kamgar, C.-C. M. Yeh, Y. Zhu, S. Gharghabi, C. A. Ratanamahatana, Yanping, B. Hu, N. Begum, A. Bagnall, A. Mueen, and H.-M. Batista, Gustavo, "The ucr time series classification archive," October 2018.
- [33] A. Bhatnagar, P. Kassianik, C. Liu, T. Lan, W. Yang, R. Cassius, D. Sahoo, D. Arpit, S. Subramanian, G. Woo *et al.*, "Merlion: A machine learning library for time series," *arXiv preprint arXiv:2109.09265*, 2021.
- [34] A. Lavin and S. Ahmad, "Evaluating real-time anomaly detection algorithms—the numenta anomaly benchmark," in *2015 IEEE 14th International Conference on Machine Learning and Applications (ICMLA)*. IEEE, 2015, pp. 38–44.
- [35] H. Xu, W. Chen, N. Zhao, Z. Li, J. Bu, Z. Li, Y. Liu, Y. Zhao, D. Pei, Y. Feng *et al.*, "Unsupervised anomaly detection via variational auto-encoder for seasonal kpis in web applications," in *Proceedings of the 2018 World Wide Web Conference*, 2018, pp. 187–196.
- [36] K. Hundman, V. Constantinou, C. Laporte, I. Colwell, and T. Soderstrom, "Detecting spacecraft anomalies using lstms and nonparametric dynamic thresholding," in *Proceedings of the 24th ACM SIGKDD international conference on knowledge discovery & data mining*, 2018, pp. 387–395.
- [37] B. Schölkopf, R. C. Williamson, A. J. Smola, J. Shawe-Taylor, J. C. Platt *et al.*, "Support vector method for novelty detection," in *NIPS*, vol. 12. Citeseer, 1999, pp. 582–588.
- [38] F. T. Liu, K. M. Ting, and Z.-H. Zhou, "Isolation forest," in *2008 eighth IEEE international conference on data mining*. IEEE, 2008, pp. 413–422.
- [39] S. Guha, N. Mishra, G. Roy, and O. Schrijvers, "Robust random cut forest based anomaly detection on streams," in *International conference on machine learning*. PMLR, 2016, pp. 2712–2721.
- [40] H. Ren, B. Xu, Y. Wang, C. Yi, C. Huang, X. Kou, T. Xing, M. Yang, J. Tong, and Q. Zhang, "Time-series anomaly detection service at

microsoft,” in *Proceedings of the 25th ACM SIGKDD International Conference on Knowledge Discovery & Data Mining*, 2019, pp. 3009–3017.

- [41] P. Malhotra, A. Ramakrishnan, G. Anand, L. Vig, P. Agarwal, and G. Shroff, “Lstm-based encoder-decoder for multi-sensor anomaly detection,” *arXiv preprint arXiv:1607.00148*, 2016.
- [42] D. P. Kingma and J. Ba, “Adam: A method for stochastic optimization,” *ICLR*, 2015.
- [43] S. Elsayed, D. Thyssens, A. Rashed, H. S. Jomaa, and L. Schmidt-Thieme, “Do we really need deep learning models for time series forecasting?” *arXiv preprint arXiv:2101.02118*, 2021.

APPENDIX

This section provides the details and hyper-parameters for COCA time series AD.

A. Detailed algorithms of COCA

First, a pseudo-code for COCA in Pytorch style is provided in Algorithm 1.

Algorithm 1 COCA’s main training algorithm.

Input: a set of augmented time series (jittering and scaling) $\{\mathbf{X}_i\}_{i=1}^N$, batch size N , structure of f, g, h, p , constant $nu, v, \gamma, \varepsilon, \lambda, \mu$.

Output: Parameters of the network f, g, h , and p .

```

for sampled batch  $\{\mathbf{X}_i\}_{i=1}^N$  do
  for all  $i \in \{1, \dots, N\}$  do
    # representations
     $\mathbf{Z}_i = f(\mathbf{X}_i)$ 
     $q_i = p(\mathbf{Z}_i)$ 
    # reconstruction representations
     $\mathbf{Z}'_i = h(g(\mathbf{Z}_i))$ 
     $q'_i = p(\mathbf{Z}'_i)$ 
     $Ce = \frac{1}{2N} \sum_{i=1}^N (q_i + q'_i)$ 
    define  $\text{sim}(u, v)$  as  $\text{sim}(u, v) = u^T v / \|u\|_2 \|v\|_2$ 
    for all  $i \in \{1, \dots, N\}$  do
      # anomaly score
      define  $S_i(\mathbf{X}_i)$  as  $2 - \text{sim}(q_i, Ce) - \text{sim}(q'_i, Ce)$ 
    if soft-boundary then
       $L = \text{quantile}(S(\mathbf{X}), 1 - \eta)$ 
       $d(Q, Q') = L + \frac{1}{vN} \sum_{i=1}^N \max\{0, S_i - L\}$ 
    else
       $d(Q, Q') = \frac{1}{N} \sum_{i=1}^N S_i(\mathbf{X}_i)$ 
       $v(Q) = \frac{1}{N} \sum_{i=1}^N \max\{0, \gamma - \sqrt{\text{Var}(q_i)} + \varepsilon\}$ 
       $v(Q') = \frac{1}{N} \sum_{i=1}^N \max\{0, \gamma - \sqrt{\text{Var}(q'_i)} + \varepsilon\}$ 
       $\mathcal{L} = \lambda d(Q, Q') + \frac{\mu}{2} (v(Q) + v(Q'))$ 
      update networks  $f, g, h$ , and  $p$  to minimize  $\mathcal{L}$ 
    return network  $f, g, h$ , and  $p$ 

```

B. Hyperparameters Details

COCA is implemented in PyTorch, and here lists some important parameter values used in the model in Table IV. In this table, *repre_channels* is the dimension of the final representations \mathbf{Z} , *hidden_size* is the dimension of the Seq2Seq in the model, and *project_channels* is the dimension of the projector. *window_size* is the size of time window, the same

as the length of time-series T , and *time_step* is the step while sliding. *stop_change_center* is the training epoch e before stopping updating the center Ce . *lr* is the learning rate and *nu* is the hyper-parameter $v \in (0, 1]$ of *soft-boundary invariance*. *scale_ratio* and *jitter_ratio* are the rate of scaling and jittering while applying data augmentation, respectively.

	NAB	AIOps_size	UCR	SMAP
repre_channels	64	32	64	32
hidden_size	128	64	128	64
project_channels	400	310	400	400
window_size	32	16	64	32
time_step	32	16	64	32
stop_change_center	10	10	10	2
lr	0.0003	0.0003	0.0003	0.0003
nu	0.001	0.01	-	-
scale_ratio	0.8	0.8	0.8	1.5
jitter_ratio	0.35	0.3	0.2	0.4

Table IV: The values of parameter used in COCA